batteries

MDPI

Article

Active Battery-Health Diagnostics for Real-World Applications Using a Bi-Directional Charger

Tim Meulenbroeks [1,2,*], Thomas Köhler [1], Md. Mahamudul Hasan [3,4], Frédéric Reymond-Laruina [5], Thomas Geury [3,4], Omar Hegazy [3,4] and Steven Wilkins [1,2]

1 Department of Powertrains, TNO, 5708 JZ Helmond, The Netherlands
2 Department of Electrical Engineering, Eindhoven University of Technology, 5600 MB Eindhoven, The Netherlands
3 MOBI-EPOWERS Research Group, ETEC Department, Vrije Universiteit Brussel, 1050 Brussel, Belgium
4 Flanders Make, Gaston Geenslaan, 3001 Heverlee, Belgium
5 EDF R&D—Electrical Equipment Laboratory, EDF Lab Les Renardières, 77250 Ecuelles, France
* Correspondence: tim.meulenbroeks@tno.nl

Abstract

Battery health data from real-world applications are vital for optimizing and predicting battery lifetime. This study presents the design and verification of an active battery-diagnostic system and method to collect such data. The system measures battery pack capacity and resistance by applying a diagnostic protocol via a bi-directional charger. This was demonstrated on a stationary-energy-storage application, under real-world conditions, to verify the system's design requirements. Measurements at the start and the end of the demonstration period of a month resulted in an observed degradation of 1.79 ± 0.34% battery capacity and an increase of 1.42 ± 0.75% in battery resistance. The successful measurements of capacity and resistance prove the compatibility of the system with real-world battery systems and confirm the design requirements were met. The system was able to perform autonomous and in situ measurements while only requiring the addition of software to the battery management system and by using the bi-directional charger of the energy storage system. By repeatedly applying the same diagnostic protocol over time, this system enables consistent tracking of battery health.

Keywords: battery health diagnosis; real-world applications; diagnostic system design; bidirectional charger; battery energy storage system

Check for updates

Academic Editor: Xianglin Li

Received: 19 February 2026
Revised: 7 April 2026
Accepted: 10 April 2026
Published: 21 April 2026

Copyright: © 2026 by the authors. Licensee MDPI, Basel, Switzerland. This article is an open access article distributed under the terms and conditions of the Creative Commons Attribution (CC BY) license.

1. Introduction

A common way to improve battery sustainability and cost is to extend battery lifetime. By extending battery lifetime, the application can realize more energy throughput for the same resource investment and CO_2 exhausted during the manufacturing of the battery. The same holds for cost; by extending battery lifetime, the depreciation of the initial investment is spread over a longer period of time, lowering the depreciation rate. To effectively extend battery life, an understanding of battery degradation under real-world conditions is important. Therefore, there is a need for battery health data from real-world applications [1].

Methods for obtaining battery health data, defined in this study as battery pack capacity and electrical resistance, have been reviewed at length in the literature [2–6]. Generally speaking, these review papers emphasize the value of battery health data from real-world applications since health data from the laboratory is usually obtained

under more strictly controlled conditions, which do not always capture real operating conditions [7,8]. As such, there is a crucial need for more battery health measurement data from real-world applications to better understand battery degradation in practice [9].

Methods for collecting battery health data can be categorized into active- and passive-diagnostic methods. Passive-diagnostic methods are based solely on observing operation via measurements, whereas active-diagnostic methods deliberately actuate the battery in some form so as to better obtain relevant parameters. Passive battery diagnostics have been thoroughly studied and reviewed [2–6,10] but active battery diagnostics in real-world applications less so, although some methods and systems for active battery diagnostics have been published [11,12]. Still, to the best of the authors' knowledge, systems and methods for active battery diagnostics for real-world applications are rare, which also applies for the use of bi-directional charger capability within that topic. Regardless of the fundamental differences between active and passive diagnostics, it is important to note that they can function side-by-side and support each other by covering each other's weaknesses. Active diagnostics can apply specific tests and provide calibration points to support passive diagnostics, and passive diagnostics can provide model-based adjustments, for measurement error and test conditions, to support active diagnostics.

Implementation-wise, passive diagnostics require little besides software but lack actuation, which can make observability of parameters challenging as it is not possible to influence the input data [13]. In contrast, active diagnostics require additional hardware and software but have the potential for reliable and repeatable testing of battery packs since the current and voltage can be directly controlled [11]. The actuation for active diagnostics can be performed internally within the application (i.e., such as via the balancing circuit), or from external systems (i.e., such as via the charger). This study focuses on the latter.

The aim of this study is to design a system and method to actively diagnose the battery pack capacity and resistance of real-world applications through the use of a bi-directional charger. This is accomplished through (A) discussing implementational challenges (Section 2), (B) deriving design requirements from those challenges, (C) designing the system and method (Sections 3 and 4), and (D) demonstrating the system and method on a battery energy storage application (Sections 5 and 6). The demonstration is part of the iSTORMY project [14] and will involve battery diagnosis over a period of a month. Due to the limited duration of the demonstration, the expected degradation of the battery is limited, and so the primary goal of the demonstration is to verify the design requirements. Aligned with the design requirements, the aim is to show reliable and repeatable diagnostic tests under real-world conditions can be performed, and that quality battery health data at the pack level can be gathered. As a final step, the future potential of the system and method is discussed from the viewpoint of large-scale long-term adoption of the system and as a tool to harvest large quantities of battery health data of real-world applications.

2. Challenges

Applying active battery diagnostics to real-world applications via a bi-directional charger comes with challenges in both system design and methodology, which are summarized in Table 1. These challenges become clear when trying to take the most straightforward approach: applying the proven and well-developed active-diagnostic methods from the laboratory directly to the application. Unfortunately, direct application is often not possible, and these methods have to be made compatible with the limitations of real-world applications to function. To illustrate this, the example is used of a commonly performed battery cell discharge-capacity test, the steps of which are summarized in Table 2 [15,16]. This well-established method cannot be directly applied to a real-world application as the laboratory discharge protocol would consist of discharging from 100% technical SoC to

0% technical SoC, as is illustrated in Figure 1a. Yet, in real-world applications, the battery manufacturer commonly applies a SoC window [17], limiting the application operation between a set range of technical SoC; in the example of Figure 1a, a 10% to 90% SoC window is applied. This makes the laboratory test impossible to apply since the BMS would shut the system down, well before 0% or 100% technical SoC would be reached. This relates to challenge C1 in Table 1.

Table 1. Challenges to apply active battery diagnostics to real-world applications that are discussed in this study.

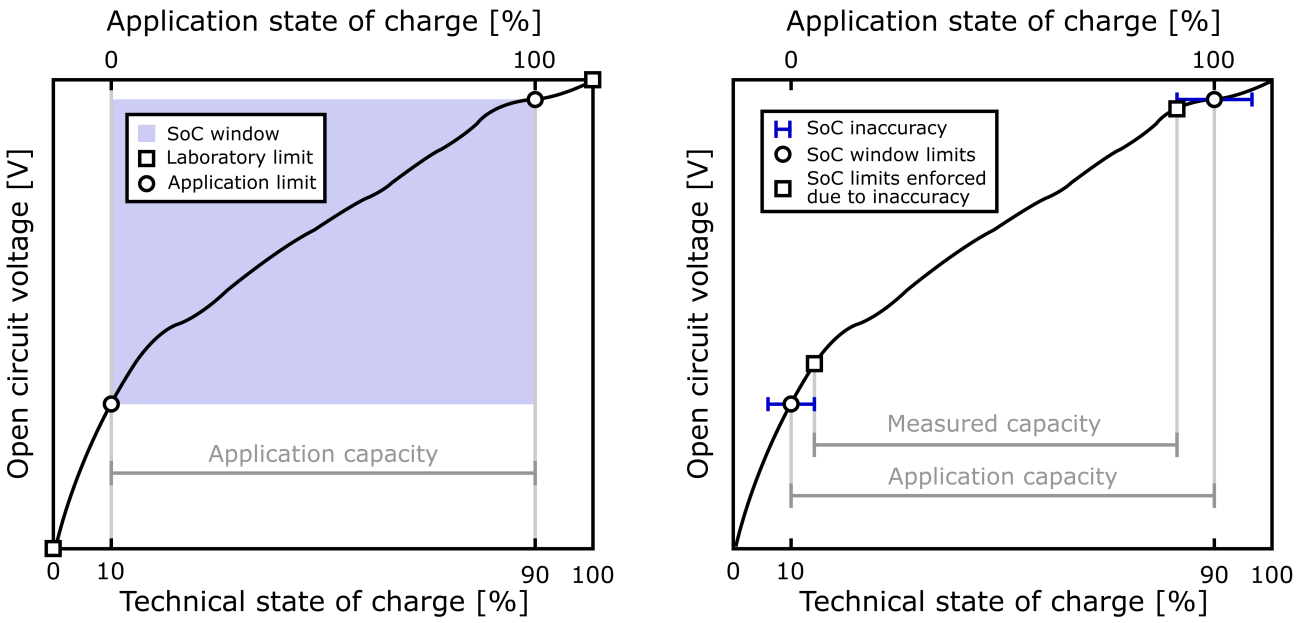
ID	Challenge	Explanation	Consequence	Links to Requirement
C1	Testing outside or near the edges of the application's SoC window causes issues.	If a SoC window is applied by the BMS, it will shut down systems and limit the battery current if measurement occurs near or outside that window.	Shutdown is an unacceptable risk to the battery user.	R1
C2	Reaching the same battery charge state consistently.	Repeatable and reliable testing depends on reaching the same battery charge state consistently. Basing the test methodology on SoC or the SoC window will make that challenging due to inaccuracy in the SoC estimation algorithm.	Inaccurate battery health data.	R2
C3	Diagnostic measurements competing with operational time.	Any time spent in diagnostic testing means the battery is not generating revenue. If diagnostic value is not in balance with the duration required for testing, the widespread adoption of the system and method will be limited	Limited scale of diagnostic system usage.	R3
C4	Building a battery-diagnostic system without adding significant initial or operating costs.	Any additional costs, like requiring additional hardware or time consuming human operations, limit widespread adoption of the system and method.	Limited scale of diagnostic system usage.	R4 + R5

Table 2. An example of a common laboratory battery cell discharge-capacity test. This test cannot be applied to any application using a SoC window because it prevents the max. and min. cell voltages from being reached (see Figure 1a).

	Description	End Criteria
1	a CC-charge is applied	until the maximum cell voltage is reached
2	a CV-charge is applied	until the cut-off current is reached
3	a CC-discharge is applied	until the minimum cell voltage is reached
4	a CV-discharge is applied	until the cut-off current is reached
Discharge capacity = The current integrated over time during step 3 and 4 Constant Current (CC) rate = C/2, Constant Voltage (CV) cut-off current = C/20		

An alternative to laboratory methods is the use of the test methodology described in the ISO-12405 standard, which defines a method to measure battery pack capacity in electric vehicles [18]. Using the example of a capacity test again, the ISO-12405 standard defines battery pack capacity as "Total number of ampere hours that can be withdrawn from a fully charged battery pack under specified conditions". In the example shown in Figure 1b "full" would translate into 90% technical SoC and "empty" to 10% technical SoC. The challenge lies in how consistently "full" and "empty" can be reached. If the target is to discharge the battery until 10% SoC is reached, but it would underestimate the SoC by 1% due to inaccuracy of the SoC algorithm, it would mean that the discharge would be stopped at 11% SoC, and the measured capacity would therefore be smaller than the

actual application capacity. If this inaccuracy varies over time, it would cause a variation in measured capacity which is completely independent of the actual degradation of the battery cell. Therefore, reaching the same battery charge state consistently is crucial to an accurate measurement of battery capacity degradation. This relates to challenge C2 in Table 1.



(**a**) (**b**)

Figure 1. (**a**) Visualisation of challenge C1 from Table 1. Applying the laboratory capacity test from Table 2 is usually not possible in real-world applications due to the widespread implementation of the SoC window; (**b**) Visualisation of challenge C2 from Table 1. Capacity measurement methods based on SoC will be affected by SoC algorithm inaccuracy.

In the study of Thingvad et al. [11], all challenges described in Table 1 play a role. In this study, the battery pack capacities of multiple electric vehicles are actively diagnosed through their use and uni-directional charging. The batteries are discharged through driving and heating until 6% application SoC is reached, after that the lights are used "until the battery reaches approx. 3% SoC". After discharging, the battery pack is fully charged, during which the capacity is measured. The fact that it was not possible to reach 0% application SoC illustrates challenge C1, and the use of the words "approximately 3% SoC" illustrates challenge C2, which implies that it is challenging to reach the same battery charge state consistently. The discharging process described by Thingvad et al. has the benefit of requiring only a uni-directional charger but has the downside of time-consuming steps and necessary human effort for driving and slow discharging through using lights and heating systems. This affects the appeal of the method in real-world applications. It is important for the widespread adoption of the method to balance these costs in terms of time and human effort with the diagnostic value gained. This relates to challenges C3 and C4 in Table 1.

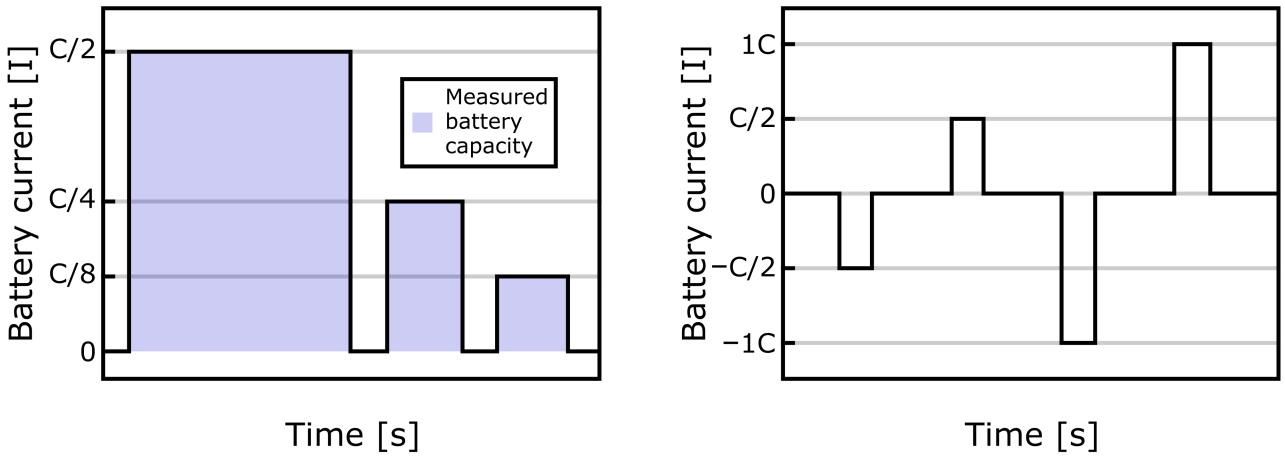
Challenge C4 is further illustrated by the work of Doan et al. [12]. In this study, battery state of health (SoH) is estimated by applying online electrochemical impedance spectroscopy. To enable these methods, the addition of specialized power electronics is necessary to inject the current waveforms of multiple different frequencies required to perform EIS. The potential of this type of active diagnosis has been shown in the literature [12]; however, the additional costs attached to the additional power electronics is an additional challenge to the widespread adoption of such systems.

3. Methods

Battery capacity and resistance were measured in this study by applying an active-diagnostic protocol to the battery pack and analyzing the resulting battery measurements. A single battery health measurement consisted of applying the diagnostic protocol exactly once and will be referred to as a diagnostic cycle. The diagnostic protocol is a sequence of experimental steps which are described in Section 3.1, and the analysis performed to convert the resulting battery measurements into battery health results is described in Section 3.2. The definitions of battery pack capacity and internal resistance which form the basis of the diagnostic protocol are described in Section 3.3. The requirements and design that shaped the diagnostic protocol and the system for applying it are discussed in Section 4.

3.1. Active-Diagnostic Protocol Specification

The aim of the active-diagnostic protocol is to measure battery pack capacity and internal resistance. The complete diagnostic protocol consisted of charge, discharge and rest steps and was split into two periods: one period to measure battery pack capacity, the other period to measure battery pack resistance. The capacity measurement protocol consisted of three constant-current-stepped profiles, as shown in Figure 2a. These three steps scan the capacity in a partial terminal-voltage range between 3.5 V and 3.9 V [19–21]. The resistance measurement protocol consisted of three sets of alternating discharge and charge CC pulses, as shown in Figure 2b, at different SoC levels within the 3.5 V–3.9 V range. To start the diagnostic protocol, it was required for the maximum battery cell voltage in the pack to be below 3.85 V, to ensure consistent battery internal states after the first capacity sub-protocol.



(**a**) (**b**)

Figure 2. (**a**) The capacity diagnostic sub-protocol. Current pulses end after any of the cell voltages reach the target voltage. All rest periods in the sub-protocol are 10 s. Partial battery pack capacity is measured by summing the charge transferred by all three current pulses; (**b**) The resistance diagnostic sub-protocol. Current pulse duration is 10 s and rest duration is 10 min. This sub-protocol is applied three times at different SoC levels to measure battery pack resistance on a 10-s timescale.

3.1.1. Capacity Diagnostic Sub-Protocol

The part of the diagnostic protocol that measured battery pack capacity consisted of three sub-protocols. Each sub-protocol had the same CC-stepped profile shape, as is depicted in Figure 2a. The first and third sub-protocol charged the battery pack, and the second sub-protocol discharged the battery pack. Every CC-phase ended when the maximum cell voltage in the pack reached 3.9 V when charging, or ended when the minimum cell voltage in the pack reached 3.5 V when discharging. After each CC-phase

a rest phase of 10 s followed. The C-rates applied were C/2, C/4 and C/8 in that order, where C is defined in this study as the nominal capacity of the battery pack, which was 250 Ah in the case of the iSTORMY demonstration (see Section 5 for details).

3.1.2. Resistance Diagnostic Sub-Protocol

The part of the diagnostic protocol that measured battery pack resistance consisted of three identical sub-protocols. Since the resistance part of the diagnostic protocol started after completion of the capacity part, the battery charge state at the start of the resistance measurement was at the top of the charge window scanned by the capacity protocol, at a terminal voltage just below 3.9 V. The resistance protocol scanned the resistance at three different charge levels by repeating the following sequence three times: discharging 25% of the capacity measured by the capacity protocol, resting for 10 min, and then applying the resistance sub-protocol shown in Figure 2b, effectively measuring resistance at 75%, 50% and 25% of the capacity range scanned by the capacity measurement. The duration of the current pulses was 10 s, and the rest duration in between was 10 min. The applied amplitudes were C/2 and 1C in alternating current directions.

3.2. Analysis Methods

3.2.1. Capacity Calculation

The battery pack charge and discharge capacity were calculated by integrating the current over time across all three stepped CC sections of the capacity sub-protocol, as depicted in Figure 2a and Equation (1). The second capacity sub-protocol was used to calculate the battery pack discharge capacity, and the third capacity sub-protocol was used to calculate the battery pack charge capacity. Note that the capacities calculated in this way represent the capacity within the battery charge range scanned by the active-diagnostic protocol. They do not represent the total capacity of the application, nor do they represent the theoretical capacity available to the user if the SoC window were not applied.

$$Q = \int_{t_{start_C/2}}^{t_{end_C/2}} I(t)\,dt + \int_{t_{start_C/4}}^{t_{end_C/4}} I(t)\,dt + \int_{t_{start_C/8}}^{t_{end_C/8}} I(t)\,dt \quad (1)$$

3.2.2. Resistance Calculation

The battery pack resistance was calculated by dividing the change in battery pack voltage by the change in battery pack current as a result of the current pulses of the resistance diagnostic sub-protocol (see Equation (2)). The period over which the change in current and voltage was observed started one second before the pulse started until and included the time that the pulse ended. Note that this resistance represents the resistance of the battery pack on a ten-second timescale only and does not reflect the resistance caused by the battery physics slower than ten seconds.

$$R = \frac{\Delta V}{\Delta I} = \frac{V_{pack_max} - V_{pack_min}}{I_{pack_max} - I_{pack_min}} \quad (2)$$

3.2.3. Degradation Calculation

The degradation of battery capacity and resistance over time was calculated by absolute and relative comparison between the measurement results of two diagnostic cycles (see Equation (3)). Since the diagnostic protocol measures both discharge and charge capacity, the total capacity degradation is taken as the mean degradation of charge and discharge capacity. All factors that affect measured battery capacity and resistance that are (partly) outside of the control of the diagnostic system but are unrelated to permanent degradation [22], like battery temperature and cell voltage imbalance, are listed in the

Results Section and/or compensated for. The degradation caused by the diagnostic protocol itself is included in the degradation measurement, although its effect is likely relatively small compared to normal operation since the intended use of the system is a single diagnostic cycle per month.

$$\Delta Q = \frac{Q_{t_2} - Q_{t_1}}{Q_{t_1}} * 100\% \qquad \Delta R = \frac{R_{t_2} - R_{t_1}}{R_{t_1}} * 100\% \qquad t_1 < t_2 \tag{3}$$

3.2.4. Measurement Uncertainty Calculation

The uncertainty estimation of the capacity measurement is based on the accuracy of the current sensor in the battery system as it is considered the most significant contributor. The sensor is of the current transducer type and the offset error, gain error and linearity error of the sensor are considered. The calculated offset error depends on the battery temperature, and the gain and linearity error depend on the mean current amplitude during measurement. The uncertainty estimation of the resistance measurement is based on the battery pack voltage sensor accuracy and the same current sensor accuracy as that for the capacity measurement.

3.2.5. Temperature Compensation Calculation

The compensation of the capacity and resistance results for the effect of temperature was calculated based on an equivalent circuit battery cell model created in the iSTORMY project. All capacity and resistance results of the 31st of October 2024 were compensated for the temperature difference of the battery compared to the 1st of October 2024. Simply put, compensation was applied by entering the observed temperatures into the model, observing the relative differences in model output and multiplying the capacity and resistance results with a factor calculated based on those differences. The resistance compensation calculation is described in Equation (4), where i is the current pulse number, n is the total number of pulses, c_1 is the cycle of 1 October, c_2 is the cycle of 31 October, and $R_{initial,c_2}$ is the resistance result of 31 of October prior to compensation. Battery temperatures during each individual pulse were entered into the battery model to calculate the compensation factor.

$$R_{compensated,c_2} = R_{initial,c_2} * f_{compensation,R} = R_{initial,c_2} * \frac{1}{n} \sum_{i=1}^{n} \frac{R_{i,c_1}(T_{i,c_1})}{R_{i,c_2}(T_{i,c_2})} \tag{4}$$

The capacity compensation calculation was based on the OCV of the battery model and the change in resistance due to the difference in temperature. The capacity was compensated by calculating the difference in the SoC range that would have been scanned if the temperature had been different, under the assumption of locally linear OCV. The SoC ranges were calculated on the basis of the voltage range between 3.5 V and 3.9 V and the voltage drop across the internal resistance indicated by the battery model.

3.3. Battery Health Definitions

Battery pack health was defined in this study as battery pack capacity and internal resistance. The definition of battery pack capacity used in this study was the maximum electrical charge that can be transferred into or out of the battery without any cell voltage exceeding the range set by two open-circuit voltages. The two open-circuit voltages selected for the demonstration system were 3.5 V and 3.9 V. The definition of battery pack resistance used in this study was the change in battery pack terminal voltage divided by the applied current over a specific time period. Capacity was defined by open-circuit voltages to remove the effect of battery resistance to ensure battery pack capacity and resistance are independently defined.

It is important to note that it is very challenging to design a practically executable diagnostic protocol that measures this definition of capacity. It is nearly impossible for practical hardware and software to control the battery voltage to reach an open-circuit voltage setpoint, mainly due to the limitations of: (A) not being able to measure open-circuit voltage and (B) the charger not being able to apply infinitely small currents to reach a voltage setpoint infinitely slowly. However, the diagnostic protocol should aim to get as close to the definition as possible to limit the effect of resistance on the capacity measurement. Figure 3 illustrates how a change in resistance can cause a variation in the measured capacity independent of the degradation of capacity. Because resistance increases as the battery ages, the difference between OCV and terminal voltage grows over time if the same current is applied, visualized through the difference in areas ΔQ_{aged} and ΔQ_{new} of Figure 3. The smaller the current amplitude of the capacity diagnostic sub-protocol is at the end, the smaller the difference is between the actual voltage and the target OCV, and the smaller the variation in this difference is over time. That is why the diagnostic protocol should aim to measure the definition as closely as possible, to measure battery pack capacity as independently as possible from battery pack resistance.

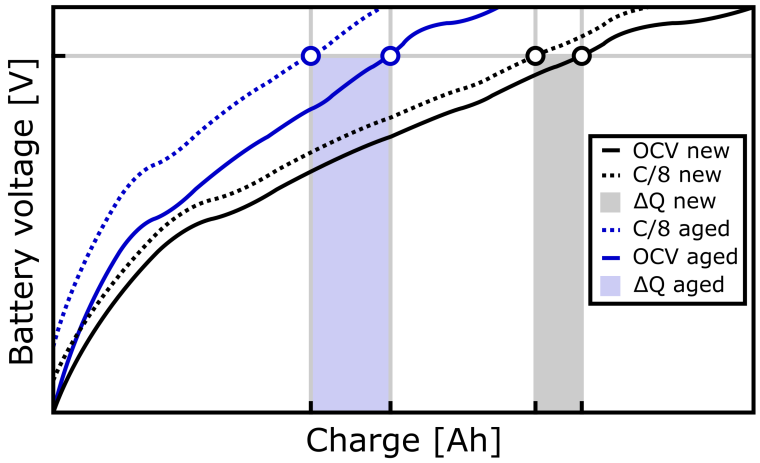


Figure 3. The effect battery aging has on the capacity measured by the diagnostic protocol. ΔQ grows as the battery ages. A battery capacity defined by open-circuit voltages is not affected by resistance increases. Therefore, the diagnostic protocol aims to measure this definition as closely as possible.

4. Design and Requirements

The design of the diagnostic protocol was motivated by solving the challenges discussed in Section 2 (see Table 1), which led to the requirements for the diagnostic system and method, summarized in Table 3. This section discusses the requirements for active diagnostics in general and the design decisions taken specifically for the diagnostic protocol and system used in the iSTORMY demonstration.

Table 3. The design requirements of the active battery-diagnostic system and method and their corresponding design decisions.

ID	Requirement	Design Decision/Specification	Applies to	Derived from Challenge
R1	The applied diagnostic protocol must operate well within the limits set by the BMS to reduce the risk of interruption.	The diagnostic protocol operates within the terminal voltage range of 3.5 V and 3.9 V. The maximum applied continuous-current amplitude is limited to C/2.	Method	C1
R2	The diagnostic protocol should be defined by setpoints expressed in a directly measurable quantity	The diagnostic protocol is defined by target voltages and currents (not SoC).	Method	C2
R3	The currents applied by the diagnostic protocol should be determined by a trade-off between time, diagnostic value, temperature increase and aging.	The current amplitudes applied by the capacity sub-protocol are C/2, C/4 and C/8. The current amplitudes applied by the resistance sub-protocol are C/2 and 1C.	Method	C3
R4	The diagnostic system should require as little additional hardware as possible to function, in order to minimize costs.	The diagnostic system uses existing hardware and only requires software to be added to the BMS.	System	C4
R5	The diagnostic system should operate as autonomously as possible, in order to minimize costs.	The only action required from the user is to start the diagnostic cycle. All other operation is automated.	System	C4

4.1. Requirement R1

Requirement R1 of Table 3 was derived from challenge C1, which states that testing outside or near the SoC window carries the unacceptable risk of shutdown. Shutdown is unacceptable from a user and operational viewpoint, but it also affects measurement repeatability and consistency. To prevent interruption, requirement R1 was created, which stated that the diagnostic protocol must operate well within the limits set by the BMS. In the case of the NMC battery pack used in the iSTORMY demonstration (see Section 5), the existing limits consisted of (A) a SoC window, (B) reduced current limits at the edges of the SoC window, and (C) temperature limits. To operate well within the SoC window and to stay away from any current or temperature limitations, the diagnostic protocol was limited to the terminal voltage range of 3.5 V and 3.9 V and a maximum continuous applied C-rate of C/2. The terminal voltage range was determined by staying at least 0.1 V away from the BMS operating limits but maximizing the range for accuracy's sake and rounding to the nearest 0.1 V. These two design decisions, limiting the operation to a terminal voltage range and limiting the maximum continuous C-rate, were taken to minimize the risk of triggering the BMS limits.

4.2. Requirement R2

Requirement R2 addresses challenge C2, which highlights the difficulty of consistently reaching the same battery charge state when using State of Charge (SoC) as a reference. To overcome this, R2 mandates that diagnostic protocol setpoints be based on directly measurable quantities, leading to the use of voltage and current targets instead of SoC. This approach enhances consistency as voltage is measured directly by a sensor, unlike SoC which relies on multiple sensor inputs and estimations. It also improves protocol standardization across different applications since voltage and current measurements are more universally harmonized than SoC estimations. As a result, the capacity diagnostic sub-protocol uses voltage-based stop criteria: charging stops when the maximum cell voltage reaches 3.9 V, and discharging stops when the minimum cell voltage reaches 3.5 V.

4.3. Requirement R3

Requirement R3 addresses challenge C3, which states that diagnostic measurements compete with operational time. The requirements states that the diagnostic protocol should consider the trade-off between (A) the protocol time duration, (B) the diagnostic value of the protocol, (C) the temperature increase due to the protocol and (D) the battery aging caused by the protocol. One approach to solving challenge C3 is to reduce the diagnostic protocol duration, which could be done by increasing the current amplitude. However, this has negative consequences for battery aging and would cause the battery temperature to increase more due to the protocol.

Considering this trade-off, the current amplitudes of the capacity sub-protocol were chosen to be C/2, C/4 and C/8. The first pulse dominates the duration of the sub-protocol; therefore, it was aligned to C/2, the highest available continuous C-rate according to requirement R1. The last pulse determined how closely the target OCV point of the battery capacity definition could be reached (see Section 3.3). To that end a lower amplitude is more favorable. However, the amplitude of C/8 was chosen as a trade-off between protocol duration and the control limits of the bi-directional charger under small loads. The C/4 step was chosen to save time between the C/2 and C/8 step. The trade-off associated with R3 is visualized in Figure 4a,b, where the trajectory of the diagnostic protocol in charge-voltage space is illustrated. They show that the diagnostic protocol can approach the capacity definition by applying an ever-diminishing current. However, this would cost an ever-increasing amount of time and would eventually run into the control limits of the bi-directional charger.

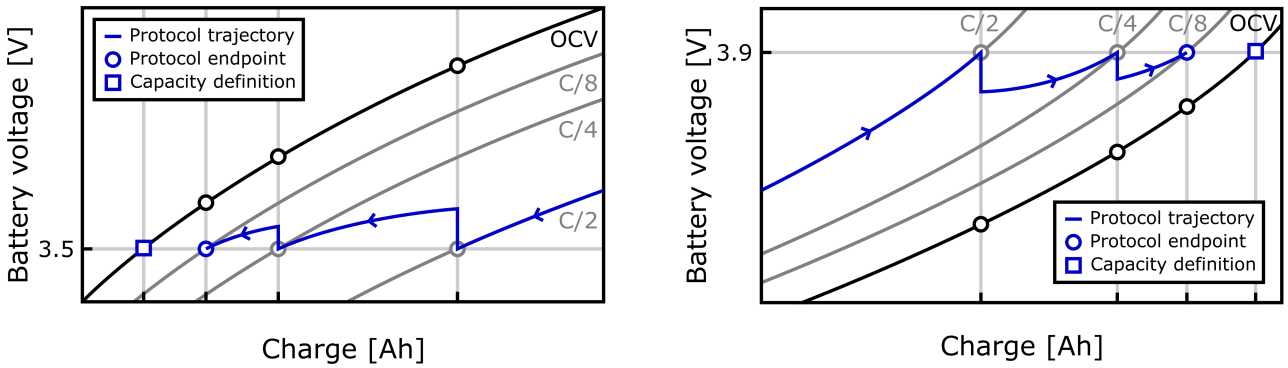


Figure 4. The trajectory of the diagnostic protocol through charge-voltage space. The protocol can measure the definition of capacity directly by applying an ever-smaller current step. However, time and charger limitations limit the minimum applied current: (**a**) at lower target voltage; (**b**) at upper target voltage.

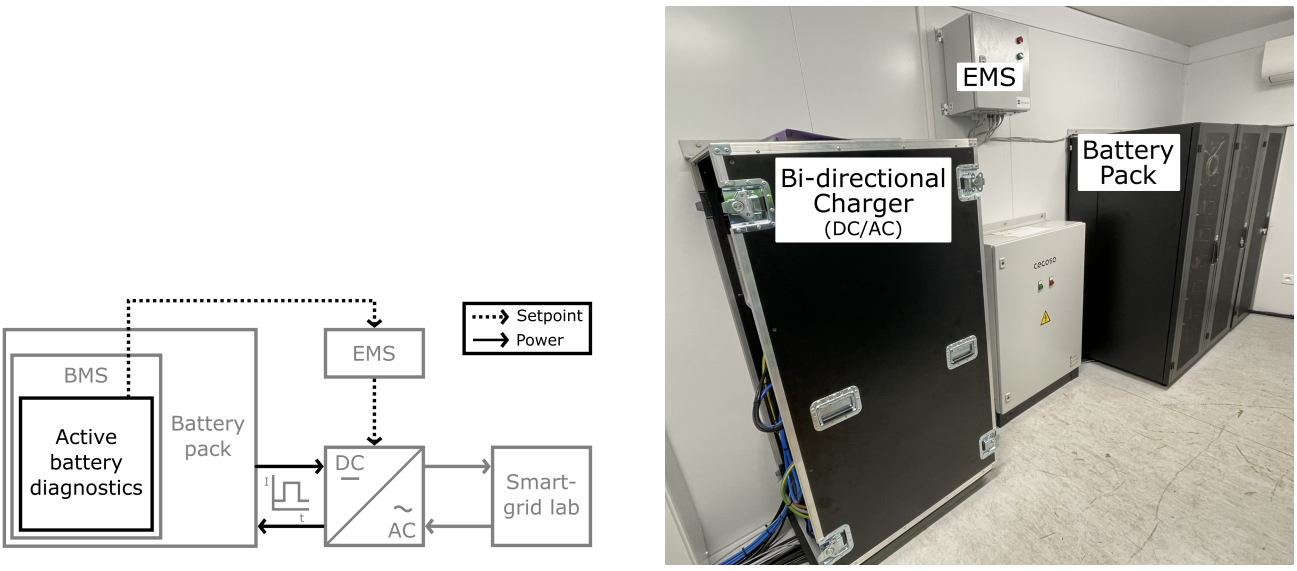
Much of the motivation for the capacity sub-protocol design choices applies to the resistance sub-protocol as well. For example, changing the SoC prior to the pulses was done at C/2 amplitude to limit protocol duration but still adhere to R1. The current rates of the current pulses were chosen to be C/2 and 1C to maximize signal to noise ratio while minimizing the risk of triggering the BMS limits and maximizing diagnostic value. The choice for three pulse sets of 4 pulses at different SoC was made to improve accuracy through multiple measurements and sweeping a representative range of SoC while keeping protocol duration in check. Alternating charge and discharge pulses were chosen to stay charge neutral over the long term, and the 10 s pulse duration was chosen to not deviate significantly away from the measured SoC point.

4.4. Requirements R4 and R5

Requirements R4 and R5 address challenge C4, which states that any additional costs required to implement and run the active diagnostics would limit the scale at which the system would be adopted. To minimize the initial cost of implementing the active diagnostics, only existing hardware in the BESS was used. This was possible in the case of the iSTORMY demonstration because the charger in a BESS is bi-directional due to the nature of the application, which suited the requirements for the active-diagnostic protocol (see Section 5 for details). To minimize operational costs, all operations of the diagnostic system were automated with the exception of the initiation of the diagnostic protocol.

4.5. System Design

The active-diagnostic system was the hardware and software that applied the diagnostic protocol to the battery pack, measured the resulting battery signals, and analyzed those signals to turn them into battery pack capacity and resistance. A schematic overview of the diagnostic system is shown in Figure 5a. The diagnostic protocol was applied by sending a power setpoint request from the active-diagnostic software running on the BMS, to the bi-directional charger, via the EMS. At the discretion of the EMS, the bi-directional charger applied the requested power to the battery pack and the BMS measured the resulting voltage, current and temperature of the battery pack. These measurements were buffered for the duration of the diagnostic cycle and after completion were used for analysis. Buffering the data locally has the advantage of having access to high-frequency, low-level measurements of the 280 individual cell voltages. An advantage of running the setpoints through the EMS, is the added level of safety. Because it has the overview of the entire BES system, it is able to (A) override or refuse any individual power setpoint or (B) to start and stop the diagnostic cycle, if deemed unsafe or unwanted.



(**a**) (**b**)

Figure 5. (**a**) A schematic overview of the iSTORMY demonstration system. The diagnostic protocol was applied by sending power setpoint requests from the diagnostics software to the bi-directional charger via Modbus; (**b**) Interior of the iSTORMY battery energy storage system (BESS) demonstrator. The active battery-diagnostic system was demonstrated on this BESS at a smart-grid laboratory.

5. Demonstration

To verify the design requirements, the active battery-diagnostic system and method were tested on the iSTORMY Battery Energy Storage System (BESS) demonstrator as part of the iSTORMY project [14]. The battery pack that was diagnosed consisted of 280 NMC 50Ah prismatic battery cells, configured in 20 modules arranged in a 4S5P configuration, with each module arranged in a 14S1P battery cell configuration. The demonstration consisted of two active-diagnostic cycles with real-world use-case tests of the BESS in between. The active-diagnostic cycles were performed on the 1st and 31st of October 2024. Due to the limited duration of the demonstration period, the expected degradation of the battery was limited, and the primary focus was to verify the design requirements. Nonetheless, the results of both diagnostic cycles were compared to assess the battery health degradation during this short period and to compare it to the estimated measurement uncertainty.

The demonstration was performed at Concept Grid, an EDF laboratory to test smart-grid solutions in a real distribution grid (see Figure 5b). Real sources and loads, such as PV inverters and EV chargers, were used in combination with power amplifiers to generate realistic scenarios. Use-case tests such as frequency support to the grid and load leveling of electric vehicle chargers were performed in between both diagnostic cycles. The combination of the facilities, the nature of the use-cases and the iSTORMY BESS created the real-world application conditions necessary to properly verify the design requirements.

6. Results

The test results of the active battery-diagnostic system of October the 1st 2024 and October the 31st 2024 are shown in Figure 6 and Figure 7, respectively. The analysis results of battery pack capacity are shown in Table 4, and the analysis results of battery pack resistance are shown in Figure 8. The analysis indicated a decrease in both discharge and charge battery pack capacity between the two dates. The capacity degradation between the test dates was 2.61 ± 0.47% for discharge capacity and was 0.83 ± 0.51% for charge capacity. Taking the mean of charge and discharge capacity resulted in a degradation of 1.79 ± 0.34%. The results of battery pack resistance show an increase in the mean battery pack resistance over time and an increase over time for every pulse set individually. The total mean battery pack resistance of all three pulse sets combined was 14.77 ± 0.08 mΩ on the 1st of October and 14.98 ± 0.08 mΩ on the 31st of October, which resulted in an increase of 1.42 ± 0.75%. The decrease in capacity and increase in resistance is in line with the expectations since the use case tests during October and the active-diagnostic cycles themselves were expected to degrade battery health during this time, if only by a little.

Important to note is that all capacity and resistance results of the 31st of October were compensated for the temperature difference compared to the 1st of October. By extension, this means that the effect of temperature on the degradation results was compensated for. The discharge capacity of October the 31st was adjusted by +0.45 Ah, the charge capacity was adjusted by +0.46 Ah, and the mean resistance of all pulses was adjusted by −0.31 mΩ.

Another notable aspect of the results is the unintended communication interruptions during the diagnostic cycle of October 1st. These were moments where the communication was interrupted between the bi-directional charger and the active-diagnostic system running on the BMS. These interruptions caused the current output to drop to zero multiple times (markers A through G in Figure 6), unintentionally relaxing the battery voltage and causing the first set of current pulses in the resistance measurement phase to be skipped.

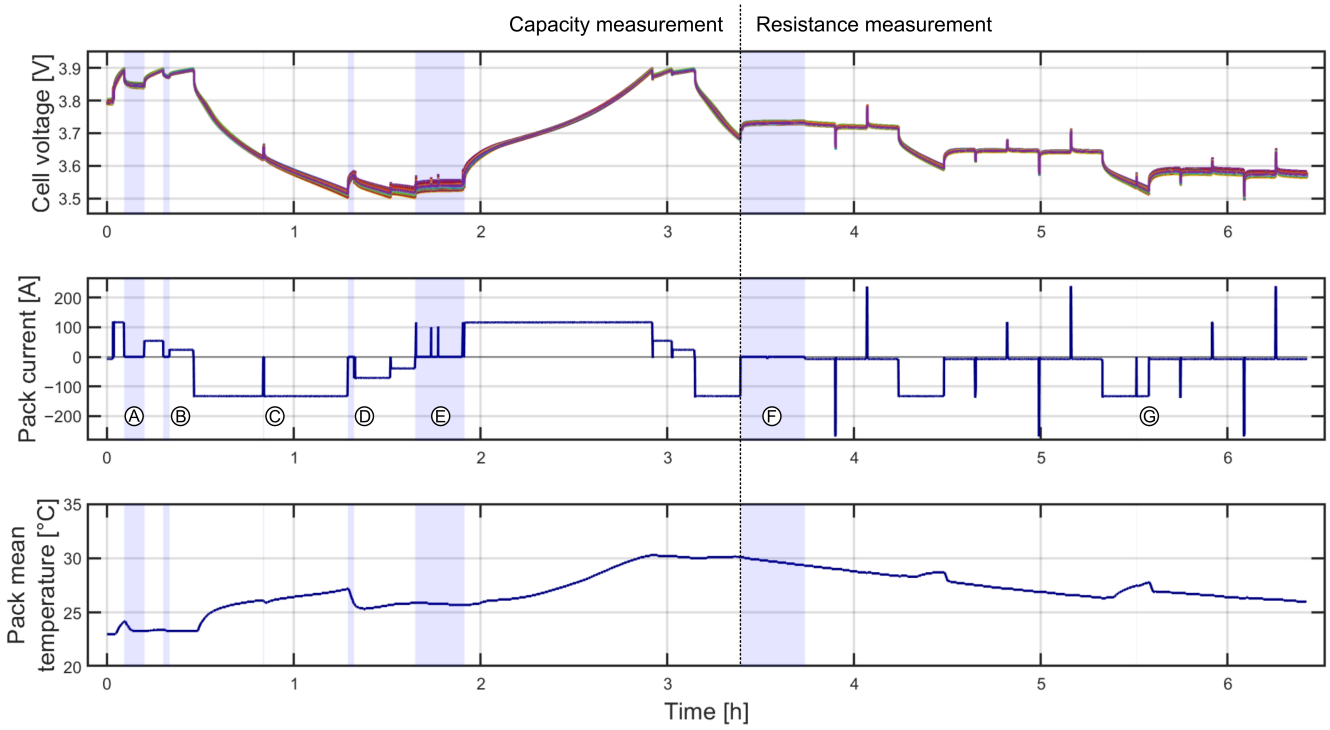


Figure 6. Results of the battery-diagnostic cycle performed on the iSTORMY BES system on the 1st of October 2024. Markers A through G indicate periods where the diagnostic protocol was interrupted due to communication loss between the active-diagnostic software and the bi-directional charger.

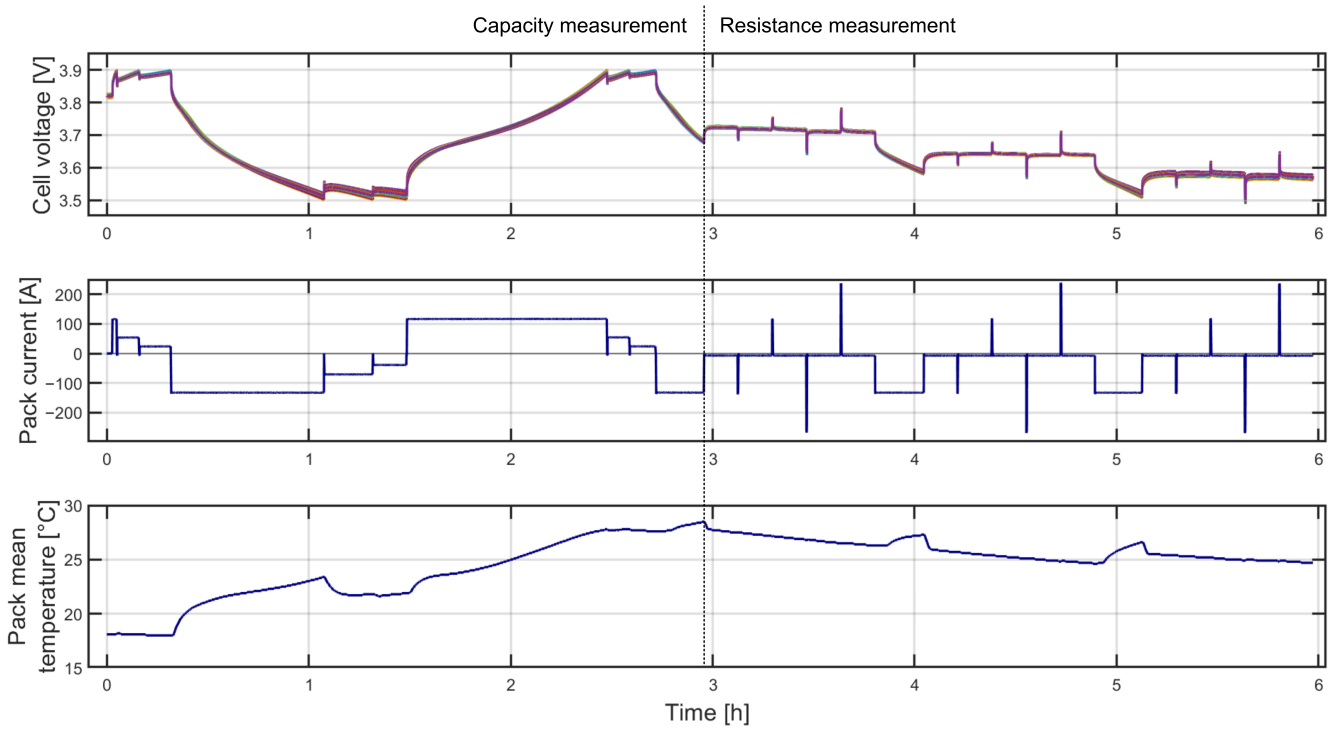
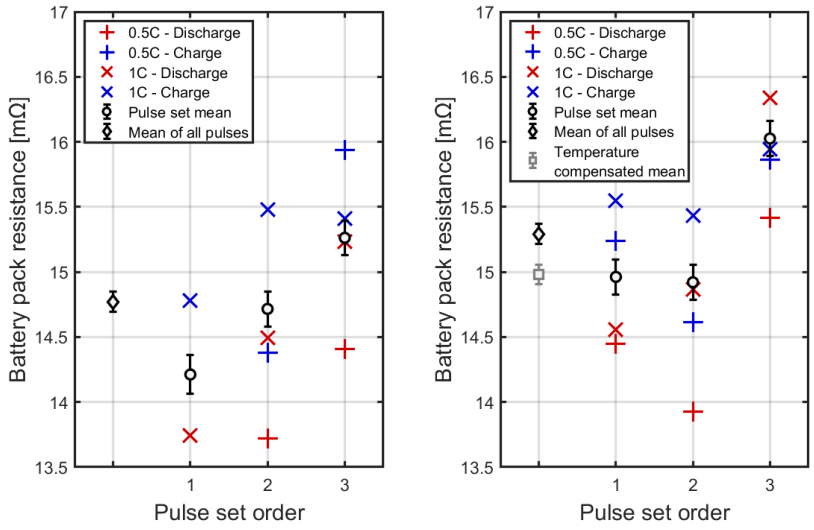


Figure 7. Results of the battery-diagnostic cycle performed on the iSTORMY BESS system on the 31st of October 2024. In contrast to the diagnostic cycle on the 1st of October, no interruptions of the protocol or the communications occurred.

Table 4. Measurement results of battery pack capacity, including the degradation between the two diagnostic cycles and a list of the conditions relevant to capacity measurement.

	1st October 2024	31st October 2024	Difference
Discharge Capacity	127.34 ± 0.43 Ah *	124.01 ± 0.42 Ah *†	−2.61 ± 0.47% *
Charge Capacity	126.12 ± 0.47 Ah *	125.07 ± 0.43 Ah *†	−0.83 ± 0.51% *
Mean			−1.79 ± 0.34% *
Conditions during the discharge-capacity measurement			
Temperature ‡	25.9 °C	21.9 °C	−4.0 °C
Min Cell Voltage ‡	3.500 V	3.500 V	+0 mV
Max Cell Voltage ‡	3.535 V	3.529 V	−6 mV
Cell Voltage Difference ‡	35 mV	29 mV	−6 mV
Conditions during the charge capacity measurement			
Temperature ‡	30.0 °C	27.6°C	−3.4 °C
Min Cell Voltage ‡	3.892 V	3.889 V	−3 mV
Max Cell Voltage ‡	3.900 V	3.900 V	+0 mV
Cell Voltage Difference ‡	8 mV	11 mV	+3 mV

* Uncertainty expressed as 1σ standard deviation based on current sensor inaccuracy. † Capacity results of 31 October were compensated based on the difference in temperature to 1 October ‡ Condition measurements taken at the last datapoint of the capacity diagnostic sub-protocol.



(**a**) (**b**)

Figure 8. The battery pack resistance results of the two diagnostic cycles: (**a**) 1st of October, (**b**) 31st of October.

6.1. Verification of Requirements

Reflecting back on the requirements presented in Table 3, in light of the results presented, reveal that all requirements were met. No interruptions of the protocol due to exceeding BMS limits occurred, satisfying requirement R1. The capacity and resistance of a battery pack in a real-world application were measured without interference of the BMS. Even though the communication interruptions of the 1st of October did affect the measurements, requirement R1 remained satisfied because they were not caused by BMS safety limit violations. Requirement R2 was also satisfied. Defining the diagnostic protocol by voltages and currents and using terminal voltages to determine when to transition between protocol steps led to a fast and simple control of the diagnostic protocol. Unfortunately, the communication interruptions still affected how consistently the same charge state could be reached, in spite of relying only on direct sensor measurements. The trade-off described in requirement R3 can be considered achieved, due to the successful capacity and resistance measurement in comparison to a total protocol duration of roughly

6.5 h and a maximum battery temperature increase of +7.3 °C and +10.5 °C on 1 and 31 October respectively. A diagnostic cycle run on a monthly basis, with relatively small time investment of 6.5 h per diagnostic cycle in exchange for a consistent measurement of battery health and all that enables, like lifetime optimization and prediction, seems a worthwhile offer to consider. Requirements R4 and R5 were satisfied because no purchase of additional hardware was necessary to run the system, and no time consuming human involvement was necessary to run the diagnostic cycle. Execution of the diagnostic protocol was fully automated with the exception of the start. These cost savings add to the appeal of the proposed active-diagnostic system and method.

To summarize, the active-diagnostic system requires relatively few resources to implement or run. The diagnostic protocol can be executed autonomously, saving human effort, and to implement the system on the application, only software needs to be added. In contrast, using the existing hardware in the application does require software adjustments to make it compatible with the diagnostics, and the dependency on the existing hardware does mean that if there are any communication interruptions or if functionality of any of the required subsystems is lost, the diagnostic system will be affected.

6.2. System and Method Performance

Reflecting back on the goals set in the Introduction Section, the results of the demonstration show that the active-diagnostic system can measure the battery pack capacity and resistance of a real-world application by using a bi-directional charger. The diagnostic cycle of the 31st of October shows that the diagnostic protocol can be applied without issue, which makes periodic consistent diagnostic cycles plausible. In contrast, the diagnostic cycle of the 1st of October does show that communication interruptions can affect operation, and care must be taken to ensure stable communication. When the diagnostic protocol is applied consistently, the C-rates, target voltages and timings of the diagnostic protocol all stay constant over time, eliminating the dependency of the battery health measurements on those factors. By repeatedly applying the same diagnostic protocol over an extended period of time, this system enables consistent tracking of battery health.

Zooming in on the performance of a specific result, the observed capacity degradation of 1.79 ± 0.34% is high compared to the expected value based on the lifetime of the battery system. The estimated measurement uncertainty does give credibility to the result, yet if the degradation is extrapolated linearly, the rate of degradation of 1.79 ± 0.34% per month would mean the battery system would degrade to 80% of initial capacity within roughly a year. Even when heavily used, the battery lifetime of a BESS of this battery type is expected to be at least multiple years. A possible explanation for this result is the fact that the battery pack was brand new at the start of the demonstration. Accelerated aging at the beginning of life has been observed in battery age tests on new cells [23], where after the initial period the degradation rate slows down. It is possible that the degradation will decrease as time progresses, and that the results solely reflect the beginning of life degradation. Another observation that can put the degradation result into perspective is the measurement uncertainty. Although a 1σ uncertainty of 0.34% indicates capacity degradation is highly likely, it is possible that the actual capacity degradation magnitude is lower than 1.79% per month.

Extrapolating the diagnostic performance beyond the scope and duration of the demonstration reveals a positive outlook. After all, the degradation results of capacity decrease and resistance increase and their uncertainties should be judged with the duration of the demonstration period in mind. A month is a relatively short time frame to observe battery degradation, but the intended use of the active-diagnostic system is monthly diagnostic cycles over the span of years. Measurements of degradation over these time

frames would have a much more favorable degradation versus uncertainty ratio. As time progresses, the magnitude of battery degradation will increase, while the measurement uncertainty will remain relatively constant, improving the ratio between them and thus the confidence in the measured degradation. Additionally, multiple diagnostic cycles would improve the statistical significance of the degradation results and decrease degradation measurement uncertainty.

In the frame of measurement performance, another result that needs to be discussed is the individual results of discharge and charge capacity degradation. The measured degradation of 2.61 ± 0.47% for discharge capacity and 0.83 ± 0.51% for charge capacity differ significantly. The exact cause of this difference could not be determined, but in all likelihood the capacity measurement was influenced by the interruptions of the protocol on the 1st of October and by extension the degradation results. The interruptions marked A and B in Figure 6 will have influenced the battery charge state at the end of the capacity sub-protocol to some extent, increasing the discharge-capacity measurement relative to the charge capacity measurement. Since no interruptions occurred on the 31st of October, this likely skewed the results, explaining the larger decrease in discharge capacity relative to charge capacity. The effect of interruptions in future use of the system would likely be smaller as the degradation would be based on multiple diagnostic cycles over a longer period, on top of the possibility of disregarding cycles that led to interruptions in the degradation analysis.

6.3. Diagnostic Protocol Improvements

The diagnostic protocol has proven to be compatible with a real-world application and has shown it is able to measure battery pack capacity and resistance. However, usage of the system has revealed that much can still be improved. Three improvement points are highlighted in the next paragraphs: (A) minimize the effects of SoC imbalance through analysis, (B) add rest periods for consistent charge-state calibration points, and (C) apply CCCV profiles whenever possible.

The first suggested diagnostic protocol improvement focuses on the effect SoC imbalance has on the measurement of battery pack capacity. Variations in SoC imbalance cause variations in measured capacity, yet any decrease in measured capacity due to SoC imbalance can be reversed, which means that it differs from permanent battery degradation. It would be beneficial to the quality of the battery health data if the contribution of permanent degradation and temporary changes could be differentiated since battery lifetime optimization only focuses on permanent degradation. Accessing control over the SoC imbalance is challenging for active diagnostics in real-world applications, so the suggested improvement is to compensate for these factors in analysis. Data-driven techniques and approaches based on the open-circuit voltage curve are prime candidates to make compensation possible.

The second suggested diagnostic protocol improvement focuses on adding rest periods to the protocol to create charge state calibration points. Even though the point of the diagnostic protocol is to improve measurement consistency by applying the same diagnostic protocol over and over again, some factors are out of its control, like the ambient temperature and the quality of sensors. Calibration points in the protocol allow for compensation for these factors, improving the quality of the battery health data. Adding rest periods at specific times in the protocol will allow the battery voltage to relax and will create opportunities to verify the battery charge state by comparison of the terminal voltage with the OCV curve. The minimum suggested improvement is to add rest periods to the end of all capacity sub-protocols to calibrate all measured capacities to the same battery charge state frame of reference (aligns with challenge C2). The expected challenge will be

to put the battery pack in true rest state, i.e., zero current flow. In real-world applications it is debatable whether this is feasible considering permanent loads like the BMS electronics.

The third suggested diagnostic protocol improvement focuses on replacing constant-current (CC) steps with constant-current constant-voltage (CCCV) steps. Figure 4a,b show that the application of an ever-smaller current allows the measurement by the protocol to approach the definition of capacity more closely, which decreases the effect the battery resistance has on capacity measurement. CCCV steps would be able to reach a smaller current in a shorter time than CC steps could, even though it would still not allow an infinitely small current to be applied as the limits of the bi-directional charger efficiency and control still exist.

6.4. Future Potential

In this study, the active-diagnostic system and method have been demonstrated on a single application for a limited period of time for verification purposes, but their potential lies in a scope larger than that. Therefore, the potential of the system and method is discussed in the scenario of large-scale, long-term use on a wide variety of applications. In terms of long-term use, the primary benefit of the system is consistent tracking of battery health. An unchanging diagnostic protocol in combination with compensation for uncontrollable factors provides a stable frame of reference to compare battery health over time. Applying the diagnostic protocol and system to other applications and battery types is, in most cases, only a matter of resizing the protocol. A change in target voltages and C-rates, aligned with the new battery specifications, is likely sufficient. As long as the diagnostic protocol does not change, a consistent comparison of results is possible for a single application. To compare the results of different diagnostic protocols between two different applications, additional analysis is required. For applications without bi-directional charger capability, like automotive, it may be more challenging due to the additional investment required for the charger, which in that case needs to be weighed against the diagnostic benefit. However, if a bi-directional charger is available, as is often the case in BES systems, scaling-up the number of active-diagnostic systems may only require software to be installed. In summary, when applied at scale, the proposed active-diagnostic system has the potential to gather vast quantities of quality battery health data cost effectively, addressing the need for battery health data from real-world applications mentioned in the Introduction Section.

7. Conclusions

The demonstration of the active-diagnostic system proves that the battery pack capacity and resistance of a real-world application can be measured by using a bi-directional charger. The diagnostic cycles performed on the iSTORMY Battery Energy Storage System (BESS) under real-world conditions verified that all the design requirements were met and showcase the method's compatibility with real-world applications. These results show that a diagnostic cycle can be applied without issues but also show that care must be taken to ensure stable communication between the diagnostic software and the charger as communication failure can disrupt consistency.

The two diagnostic cycles performed at the start and the end of the demonstration period of a month resulted in an observed degradation of 1.79 ± 0.34% in battery capacity and an increase of 1.42 ± 0.75% in battery resistance. Extrapolating these results beyond the duration of the demonstration indicates that quality battery degradation data can be harvested since measurements over a longer time frame will have a much more favorable degradation versus uncertainty ratio. As time progresses, the magnitude of battery degradation will increase, while the measurement uncertainty will remain

relatively constant, improving the ratio between them, and thus the confidence in the measured degradation.

The proposed active-diagnostic system and method offer several important advantages for harvesting battery health data from real-world applications. First and foremost, the diagnostic system and method enable consistent tracking of battery health over time. Applying the same diagnostic protocol each time and compensating for uncontrollable factors provide a stable frame of reference for comparison of battery health. Second, the system shows potential for cost-effective harvesting of battery health data due to the limited hardware requirements and limited human efforts required to operate. The operation of the system during the demonstration only required the addition of software to the BESS, and the diagnostic protocol was applied autonomously after initiation by the user. Third, the diagnostic method can be easily applied to a wide range of applications due to the adaptability of the diagnostic protocol. The combination of consistency, cost-effectiveness, and broad applicability of the diagnostic system and method all contribute to addressing the need for battery health data from real-world applications discussed in the Introduction section.

Future Research

Future research should focus on applying the diagnostic method in different types of applications and applying more diagnostic cycles for an extended duration. Doing so will allow for a more complete assessment of diagnostic measurement performance and validation of the method. To further boost measurement performance, the diagnostic protocol should be improved according to the suggestions made in this study.

Author Contributions: Conceptualization, T.M., T.K. and S.W.; methodology, T.M.; project administration, T.G. and O.H.; software, T.M. and T.K.; investigation, T.M., M.M.H. and F.R.-L.; writing—original draft preparation, T.M.; writing—review and editing, T.K., M.M.H., F.R-.L. and S.W.; funding acquisition, T.M., T.G., O.H. and S.W. All authors have read and agreed to the published version of the manuscript.

Funding: This project has received funding from the European Union's Horizon 2020 research and innovation program under grant agreement No. 963527 (iSTORMY).



Data Availability Statement: The original contributions presented in this study are included in the article. Further inquiries can be directed to the corresponding author.

Acknowledgments: The authors would like to acknowledge the iSTORMY consortium partners for supporting this study.

Conflicts of Interest: The authors declare no conflicts of interest.

Abbreviations

The following abbreviations are used in this manuscript:

BESS	Battery Energy Storage System
BMS	Battery Management System
EMS	Energy Management System
SoH	State of Health
SoC	State of Charge
OCV	Open-Circuit Voltage

C	Battery Capacity
CC	Constant Current
CV	Constant Voltage
ISO	International Organization for Standardization
NMC	Nickel Manganese Cobalt Oxide
EV	Electric Vehicle

References

1. Rücker, F.; Figgener, J.; Schoeneberger, I.; Sauer, D.U. Battery Electric Vehicles in Commercial Fleets: Use profiles, battery aging, and open-access data. *J. Energy Storage* **2024**, *86*, 111030. [CrossRef]
2. Dini, P.; Colicelli, A.; Saponara, S. Review on Modeling and SOC/SOH Estimation of Batteries for Automotive Applications. *Batteries* **2024**, *10*, 34. [CrossRef]
3. Berecibar, M.; Gandiaga, I.; Villarreal, I.; Omar, N.; Van Mierlo, J.; Van Den Bossche, P. Critical review of state of health estimation methods of Li-ion batteries for real applications. *Renew. Sustain. Energy Rev.* **2016**, *56*, 572–587. [CrossRef]
4. Pradhan, S.K.; Chakraborty, B. Battery management strategies: An essential review for battery state of health monitoring techniques. *J. Energy Storage* **2022**, *51*, 104427. [CrossRef]
5. Farmann, A.; Waag, W.; Marongiu, A.; Sauer, D.U. Critical review of on-board capacity estimation techniques for lithium-ion batteries in electric and hybrid electric vehicles. *J. Power Sources* **2015**, *281*, 114–130. [CrossRef]
6. Xiong, R.; Li, L.; Tian, J. Towards a smarter battery management system: A critical review on battery state of health monitoring methods. *J. Power Sources* **2018**, *405*, 18–29. [CrossRef]
7. Sulzer, V.; Mohtat, P.; Aitio, A.; Lee, S.; Yeh, Y.T.; Steinbacher, F.; Khan, M.U.; Lee, J.W.; Siegel, J.B.; Stefanopoulou, A.G.; et al. The challenge and opportunity of battery lifetime prediction from field data. *Joule* **2021**, *5*, 1934–1955. [CrossRef]
8. Wang, Q.; Wang, Z.; Liu, P.; Zhang, L.; Sauer, D.U.; Li, W. Large-scale field data-based battery aging prediction driven by statistical features and machine learning. *Cell Rep. Phys. Sci.* **2023**, *4*, 101720. [CrossRef]
9. Hu, X.; Xu, L.; Lin, X.; Pecht, M. Battery Lifetime Prognostics. *Joule* **2020**, *4*, 310–346. [CrossRef]
10. Li, Y.; Abdel-Monema, M.; Gopalakrishnan, R.; Berecibar, M.; Nanini-Maury, E.; Omar, N.; van den Bossche, P.; Van Mierlo, J. Erratum to 'A quick on-line state of health estimation method for Li-ion battery with incremental capacity curves processed by Gaussian filter' [J. Power Sources 373 (2018) 40–53] (S0378775317314532) (10.1016/j.jpowsour.2017.10.092)). *J. Power Sources* **2018**, *393*, 230. [CrossRef]
11. Thingvad, A.; Calearo, L.; Andersen, P.B.; Marinelli, M. Empirical Capacity Measurements of Electric Vehicles Subject to Battery Degradation from V2G Services. *IEEE Trans. Veh. Technol.* **2021**, *70*, 7547–7557. [CrossRef]
12. Doan, V.T.; Vu, V.B.; Vu, H.N.; Tran, D.H.; Choi, W. Intelligent charger with online battery diagnosis function. In *Proceedings of the 9th International Conference on Power Electronics—ECCE Asia: "Green World with Power Electronics", ICPE 2015-ECCE Asia*; IEEE: Seoul, Republic of Korea, 2015; pp. 1644–1649, ISBN 9788957082546. [CrossRef]
13. Plett, G.L. Extended Kalman filtering for battery management systems of LiPB-based HEV battery packs. *J. Power Sources* **2004**, *134*, 277–292. [CrossRef]
14. iSTORMY Project Website. Available online: https://istormy.eu/ (accessed on 21 July 2025).
15. Dubarry, M.; Baure, G. Perspective on Commercial Li-ion Battery Testing, Best Practices for Simple and Effective Protocols. *Electronics* **2020**, *9*, 152. [CrossRef]
16. Barai, A.; Uddin, K.; Dubarry, M.; Somerville, L.; McGordon, A.; Jennings, P.; Bloom, I. A comparison of methodologies for the non-invasive characterisation of commercial Li-ion cells. *Prog. Energy Combust. Sci.* **2019**, *72*, 1–31. [CrossRef]
17. Wikner, E.; Björklund, E.; Fridner, J.; Brandell, D.; Thiringer, T. How the utilised SOC window in commercial Li-ion pouch cells influence battery ageing. *J. Power Sources Adv.* **2021**, *8*, 100054. [CrossRef]
18. *ISO 12405-4:2018*; Electrically Propelled Road Vehicles—Test Specification for Lithium-ion Traction Battery Packs and Systems. ISO: Geneva, Switzerland, 2018; 72p.
19. Stroe, D.I.; Knap, V.; Schaltz, E. State-of-Health Estimation of Lithium-Ion Batteries Based on Partial Charging Voltage Profiles. *ECS Meet. Abstr.* **2018**, *MA2018-01*, 532. [CrossRef]
20. Schaltz, E.; Stroe, D.I.; Nørregaard, K.; Johnsen, B.; Christensen, A. Partial Charging Method for Lithium-Ion Battery State-of-Health Estimation. In *Proceedings of the 2019 Fourteenth International Conference on Ecological Vehicles and Renewable Energies (EVER)*; IEEE: Monte-Carlo, Monaco, 2019; pp. 1–5. [CrossRef]
21. Ahmeid, M.; Muhammad, M.; Lambert, S.; Attidekou, P.S.; Milojevic, Z. A rapid capacity evaluation of retired electric vehicle battery modules using partial discharge test. *J. Energy Storage* **2022**, *50*, 104562. [CrossRef]

22. Thingvad, M.; Calearo, L.; Thingvad, A.; Viskinde, R.; Marinelli, M. Characterization of NMC Lithium-ion Battery Degradation for Improved Online State Estimation. In *Proceedings of the 2020 55th International Universities Power Engineering Conference (UPEC)*; IEEE: Turin, Italy, 2020; pp. 1–6. [CrossRef]
23. Luh, M.; Blank, T. Comprehensive battery aging dataset: Capacity and impedance fade measurements of a lithium-ion NMC/C-SiO cell. *Sci. Data* **2024**, *11*, 1004. [CrossRef] [PubMed]

Disclaimer/Publisher's Note: The statements, opinions and data contained in all publications are solely those of the individual author(s) and contributor(s) and not of MDPI and/or the editor(s). MDPI and/or the editor(s) disclaim responsibility for any injury to people or property resulting from any ideas, methods, instructions or products referred to in the content.